Nuclear Instruments and Methods in Physics Research A 735 (2014) 1–6

Contents lists available at ScienceDirect

Nuclear Instruments and Methods in Physics Research A

journal homepage: www.elsevier.com/locate/nima

Three-dimensional SPECT imaging with $LaBr_3$:Ce scintillator for characterization of nuclear waste

Tushar Roy*, Jilju Ratheesh, Amar Sinha

Neutron & X-Ray Physics Division, Bhabha Atomic Research Centre, Trombay, Mumbai, India

ARTICLE INFO

Article history:
Received 8 July 2013
Received in revised form
3 August 2013
Accepted 6 August 2013
Available online 28 August 2013

Keywords:
3D SPECT
Lanthanum bromide
Novikov's inversion formula

ABSTRACT

Characterization of nuclear waste in terms of radioactivity distribution is important not only for their safe disposal but also for nuclear material accounting. Single Photon Emission Computed Tomography (SPECT) provides a non-invasive technique for the characterization and activity distribution of the gamma-emitting sources in a matrix. Sodium iodide scintillators, which are most commonly used, suffer from poor energy resolution and do not provide accurate peak discrimination for radioisotopes like ^{239}Pu which have overlapping peaks. Cerium-activated lanthanum bromide ($LaBr_3$:Ce) scintillators have better energy resolution and provide better peak discrimination. In this paper, experimental studies using $LaBr_3$:Ce for 3D SPECT imaging of dummy waste drum has been discussed. The reconstruction has been done using the Filtered Backprojection scheme with attenuation compensation based on Novikov's inversion formula.

1. Introduction

Characterization of the contents of nuclear waste drums is required for disposition decisions, safe transportation and permanent storage. Movement of waste drums on and off storage sites is regulated for safety and environmental reasons. Examination of contents with invasive techniques is expensive because of the safety precautions necessary when handling nuclear waste. The conventional X-ray radiography or transmission tomography techniques [1,2] do not yield information about the radioisotopes inside the drum, but just on the material density. Gamma spectroscopy in open geometry or segmented gamma scanning can be performed to this aim, but to improve accuracy and provide information about the spatial distribution of the radioisotopes, emission computed tomography (ECT) techniques are best suited.

Single Photon Emission Computed Tomography (SPECT) is a non-invasive technique for the characterization of the activity level and distribution of gamma emitting radioisotopes inside an object. It involves the measurement of gamma rays emitted by a radionuclide with a collimated detector to segment the acquisition angularly, horizontally and vertically, and thus obtain information about each voxel of the inspected volume.

The intensities of the radiation measured are directly related to the radionuclide distribution inside the object. The data is collected by translating, elevating and rotating the object over 360° , and then reconstructed using analytical or iterative techniques. These intensities are used as input to the different types of reconstruction techniques for identification of emissions from the given volume.

1.1. Lanthanum bromide scintillator

Cerium-activated lanthanum bromide ($LaBr_3$:Ce) scintillation detectors are well known for their improved energy resolution, fast emission and excellent temperature and linearity characteristics as compared to commonly used sodium iodide detectors. Typical energy resolution at 662 keV is 3% as compared to 7% for sodium iodide (NaI(Tl)) detectors [3]. The improvements in resolution allow more accurate peak discrimination in ranges where isotopes often have many overlapping peaks. This leads to better isotope classification.

The efficiency for $LaBr_3$:Ce is about 1.18 times that of NaI(Tl) for the same volume and the decay time constant is slightly more than 10% of the NaI detector decay time [4] (see Table 1). On the basis of photoelectron yield, $LaBr_3$:Ce has higher efficiency and temperature stability than NaI(Tl) (Fig. 1).

1.2. Experimental set-up

An emission tomography laboratory has been set up at Purnima Labs, BARC for 3D SPECT imaging. The experimental set-up is shown in Fig. 2. It consists of a 3-axis sample manipulator (y, z, θ), collimator–detector assembly (see details in "Results" section) and an external gamma source ^{152}Eu (for Active CT). The object is placed on the sample manipulator. The system can scan an object of maximum size 600 mm diameter and 1000 mm height (Fig. 3).

* Corresponding author. Tel.: +91 2225595492.
E-mail addresses: tushar@barc.gov.in, tusharroy17@gmail.com (T. Roy).

0168-9002/$ - see front matter © 2013 Elsevier B.V. All rights reserved.
http://dx.doi.org/10.1016/j.nima.2013.08.037

1.3. Novikov's inversion formula

In case of SPECT, the photons emitted by the radioisotope suffer attenuation inside the object. Consider a vector $\overline{x}=(x,y)$ in a two-dimensional Euclidean space. Let $f(\overline{x})$ denote the distribution of radioisotope activity and $\mu(\overline{x})$ denote the attenuation map of the surrounding object. The attenuated 2D Radon transform for parallel beam geometry is of the form [5–7]

$$g(s,\theta)=[\Re_{att}f](s,\theta)=\int_{-\infty}^{\infty}f(s\underline{\theta}+t\underline{\theta}^{\perp})e^{-\int_{t}^{\infty}\mu(s\underline{\theta}+\tau\underline{\theta}^{\perp})d\tau}\,dt \tag{1}$$

where $\overline{\theta}=\begin{pmatrix}\cos\theta\\ \sin\theta\end{pmatrix}$, $\overline{\theta}^{\perp}=\begin{pmatrix}-\sin\theta\\ \cos\theta\end{pmatrix}$ and $D_{\mu}(\overline{x},\overline{\varphi})$ is the divergent beam transform of $\mu(\overline{x})$ in the direction of $\overline{\varphi}=\begin{pmatrix}\cos\varphi\\ \sin\varphi\end{pmatrix}$ defined as

$$D_{\mu}(\overline{x},\overline{\varphi})=\int_{0}^{\infty}\mu(\overline{x}+p\overline{\varphi})dp \tag{2}$$

Table 1
Comparison of critical parameter (typical) for lanthanum bromide detectors [4].

Detector type	Resolution @662 keV (%)	Density (g/cc)	Light yield (photons/keV)	Primary decay time (ns)
$LaBr_3$:Ce	3	5.08	63	16
NaI(Tl)	7	3.67	38	250

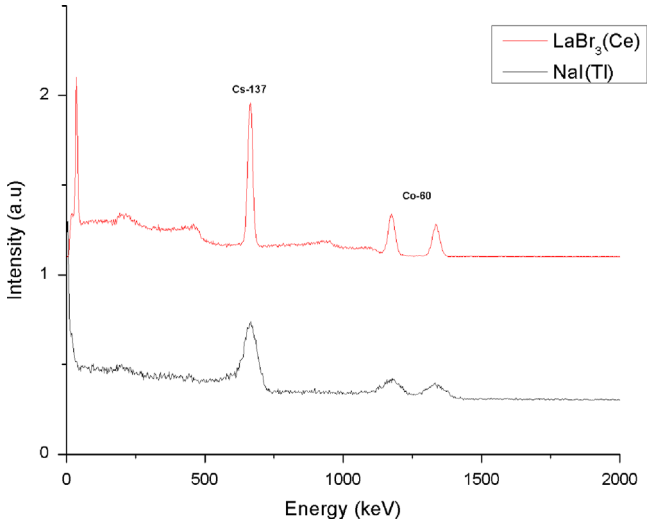

Fig. 1. Typical gamma spectrum acquired with NaI(Tl) and $LaBr_3$(Ce).

Assuming $\mu(\overline{x})$ is known, Novikov gave an explicit inversion formula to reconstruct $f(\overline{x})$ from the parallel projection data $g(s,\theta)$:

$$f(\overline{x})=\frac{1}{4\pi}\mathrm{Re}\left\{\nabla.\int_{0}^{2\pi}\overline{\theta}\{e^{-h(s,\theta)+D_{\mu}(\overline{x},-\overline{\theta}^{\perp})}He^{h(s,\theta)}g(s,\theta)\}|_{s=\overline{x}.\overline{\theta}}d\theta\right\} \tag{3}$$

where $h(s,\theta)=\frac{1}{2}(I+iH)[\Re\mu](s,\theta)$ and $[H\varphi](s,\theta)=\frac{1}{\pi}p.v.\int_{-\infty}^{\infty}\frac{\varphi(s',\theta)}{s-s'}ds'$

I is the identity operator. H is the Hilbert transform with respect to the second parameter.

2. Results

For the experiments under report, three $LaBr_3$:Ce detectors (BrilLanCe™380 1″ X 1″) have been used with specially designed SS–Pb–SS collimator (Fig. 4) with tungsten septa. The collimator opening of 26 mm is divided into four equal segments using high attenuating tungsten septa of thickness 1.6 mm. For the present experiment, two such collimators were used in series for each detector. The effective L/d ratio is 10.

To simulate a waste drum, an aluminum drum (300 mm diameter and 600 mm height) filled with cotton gloves and cotton fiber (average attenuation coefficient: 0.05 cm^{-1}) was used as an object. Three ^{137}Cs sources were placed inside the drum at different positions. Data was acquired at 12 lateral positions and 36 angular positions for each Z-position. In the vertical direction, 24 Z-positions were scanned. Thus each slice thickness is 25 mm. The acquisition time for each data is 10 s. The photopeak efficiency of $LaBr_3$:Ce detectors used in the experiment is 0.02 for the 662 keV gamma ray of ^{137}Cs.

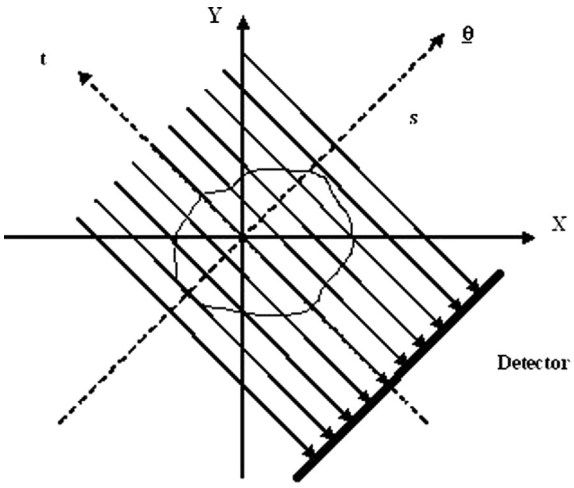

Fig. 3. Parallel beam geometry.

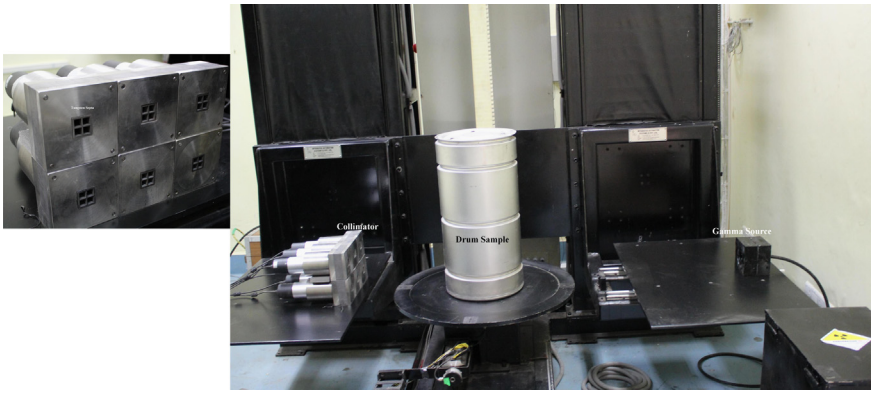

Fig. 2. Experimental set-up at Purnima Labs (Inset) Colli mator with septa.

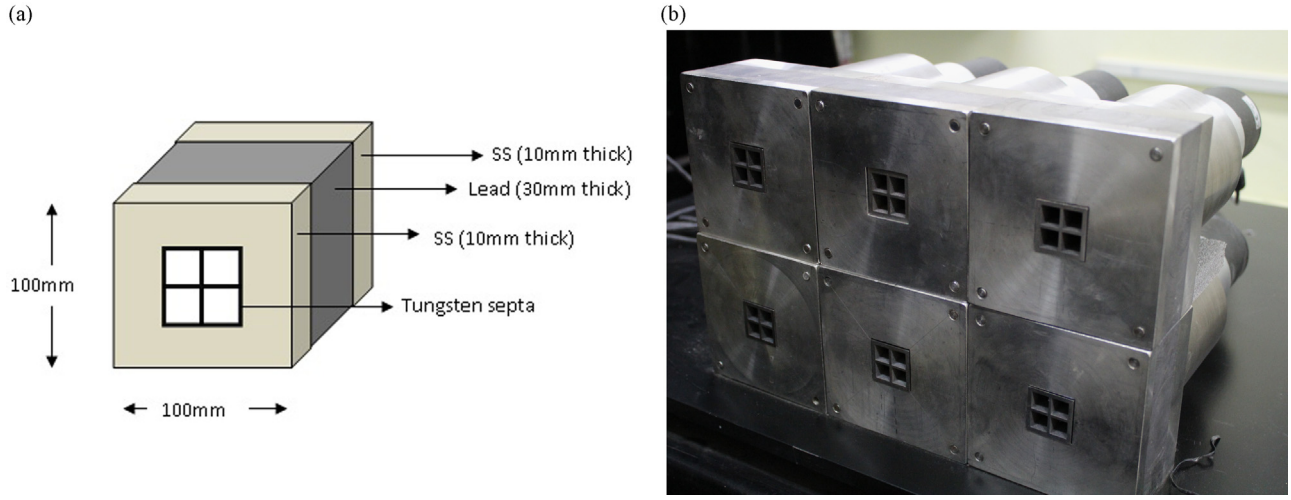

Fig. 4. (a) Schematic and (b) photograph of collimator with septa.

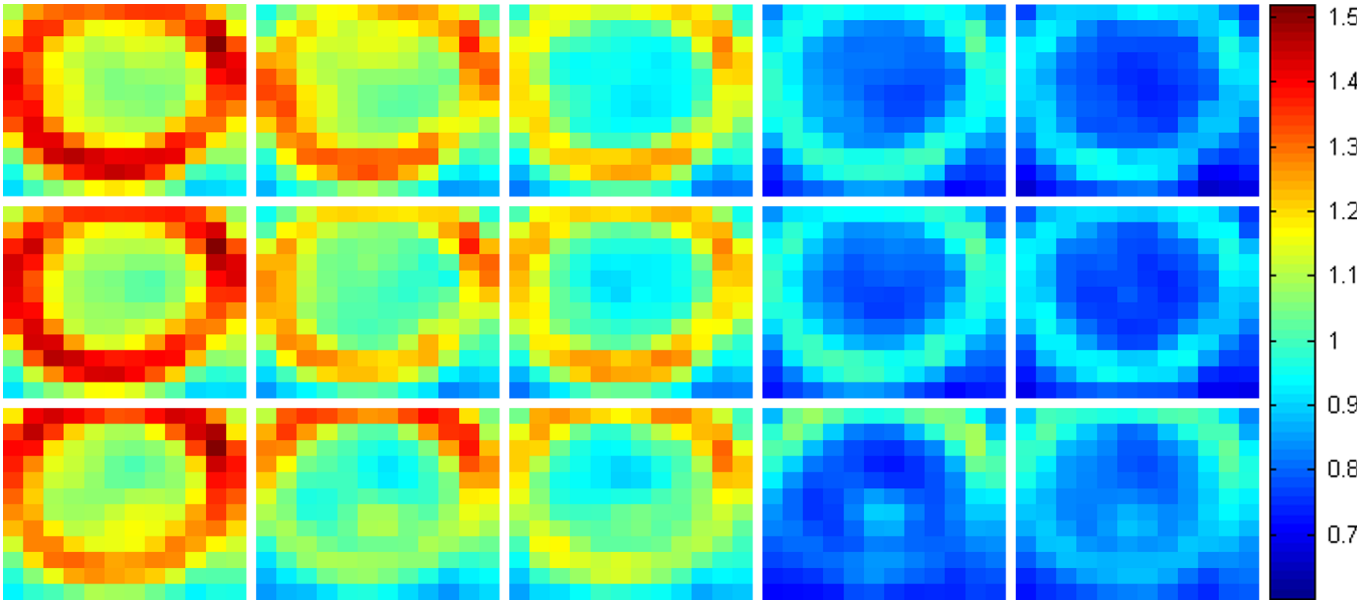

Fig. 5. TCT data for three different slices (top to bottom) at different energies (from left to right)—244 keV, 344 keV, 444 keV, 778 keV and 867 keV; color bar is shown on the right (in unit of cm^{-1}).

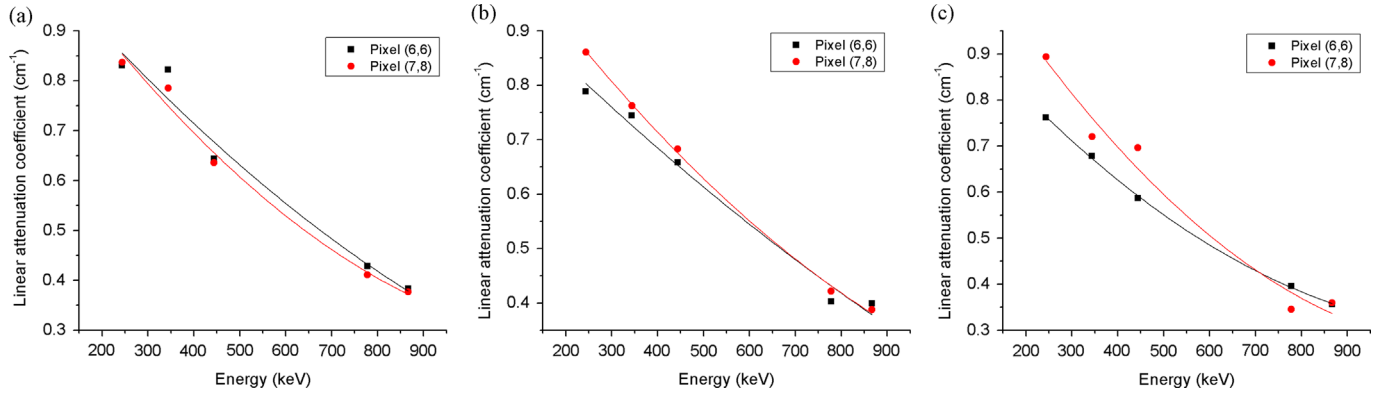

Fig. 6. Plot of linear attenuation coefficient as a function of energy for (a) top row (b) middle row and (c) bottom row of TCT data in fig. 5.

For attenuation compensation, transmission computed tomography (TCT) of the drum was carried out using Eu-152 source. The TCT data were acquired for different energies (244 keV, 344 keV, 444 keV, 778 keV and 867 keV). The attenuation map was reconstructed for each energy using FDK [8] algorithm. Fig. 5 shows the reconstructed TCT data for three slices at different energies. Fig. 6 shows the plot of

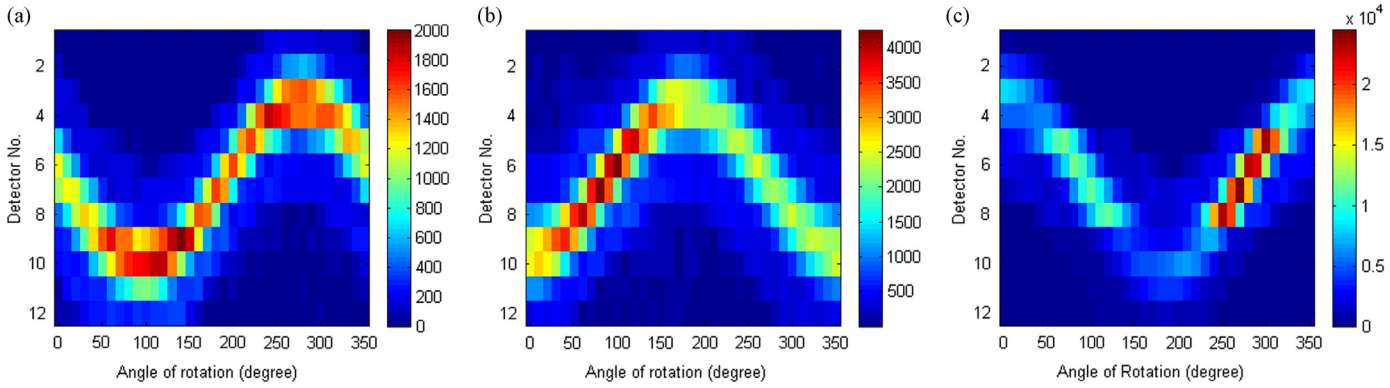

Fig. 7. Sinogram of SPECT data for (a) slice 4 (b) slice 13 and (c) slice 18.

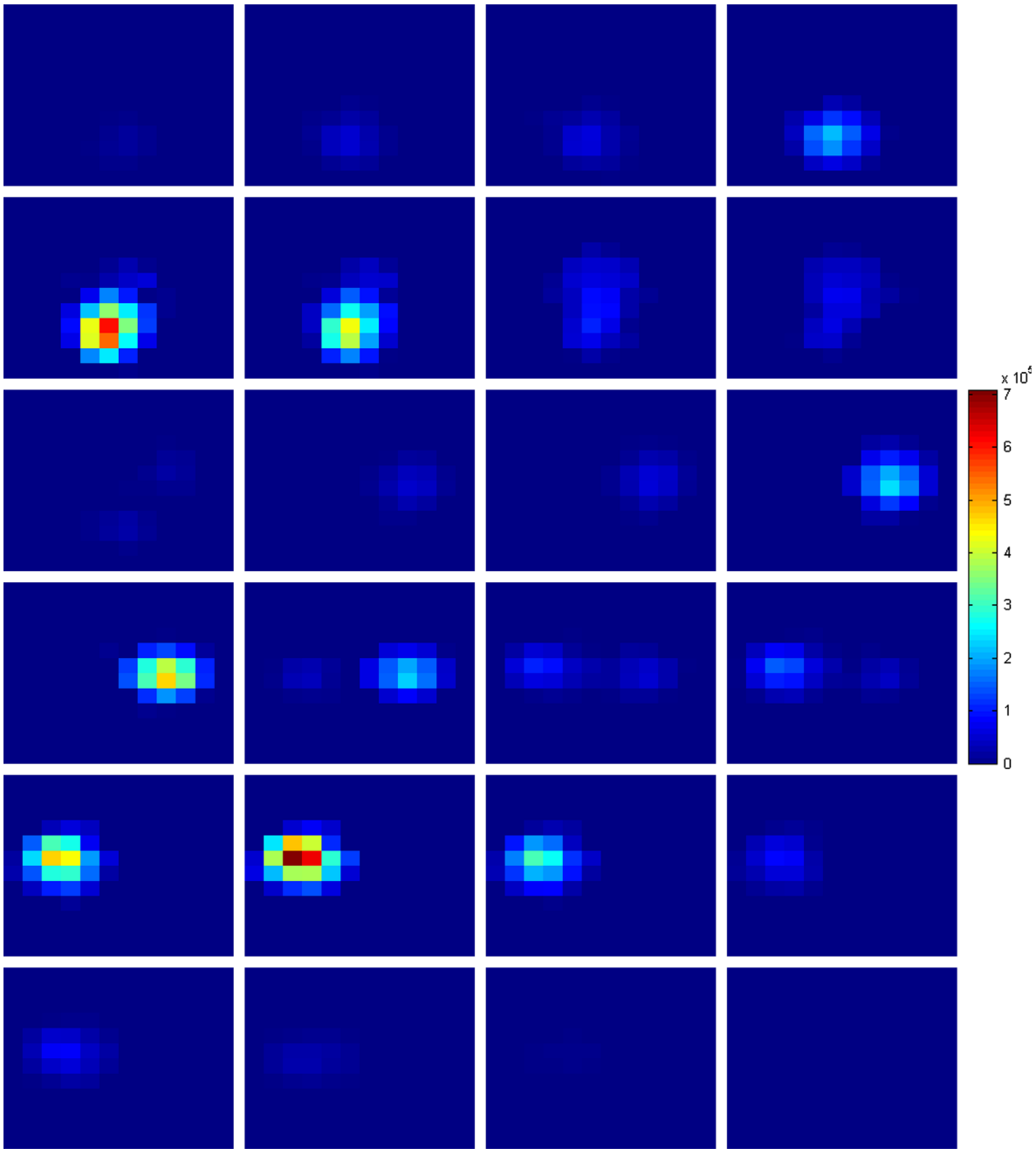

Fig. 8. Reconstructed slice images showing ^{137}Cs activity in a drum. The images show XY slices at different Z-positions starting from bottom to top (ordered row-wise left to right); Color bar shown on the right (in unit of counts per 10 s). (For interpretation of the references to color in this figure legend, the reader is referred to the web version of this article.)

attenuation coefficient as a function of energy. The attenuation map for 662 keV (emission energy in SPECT) was interpolated from these data. This attenuation map was used for attenuation compensation.

The SPECT reconstruction was done using the Filtered Backprojection scheme with attenuation compensation based on Novikov's inversion formula (Eq. 3). The reconstructed volume is discretized on a $12 \times 12 \times 24$ grid. Fig. 7 shows sinogram corresponding to three XY slices. Reconstructed XY slices at different Z-positions are shown in Fig. 8. The reconstructed 3D volume is shown in Fig. 9. For 3D volume visualization, the data was interpolated on finer grid ($30 \times 30 \times 60$). It can be seen that spatial position of the radioisotopes can be easily located. The reconstructed activity distribution in the images matches well with the true source activity in the original object (see Table 2).

The activity (in disintegrations per second) for each voxel is given by

$$A = \frac{C}{t\beta_\gamma \varepsilon} \tag{4}$$

where C is the counts in the voxel, t is the acquisition time, β_γ is the branching ratio of the emitted gamma for the particular isotope and ε is the detector efficiency. The total activity for each distinct source is calculated by summing all the voxels in the neighborhood.

Fig. 10 shows the line profiles along x-axis, y-axis and z-axis respectively for the sources. The spread in the line profiles is mainly due to the collimator blurring (and scattering) which is one

Table 2
Comparison of reconstructed and true source activity.

Source	Source position (Pixel no.)	Source position (in mm) (x, y, z)	True activity (MBq)	Reconstructed activity (MBq)	Relative error (%)
A	(10, 6, 5)	(95.5, −13.6, 112.5)	26.7	27.9	−4.5
B	(7, 9, 13)	(13.6, 68.2, 312.5)	21.0	19.5	7.1
C	(6, 3, 18)	(−13.6, −95.5, 437.5)	37.8	34.7	8.2

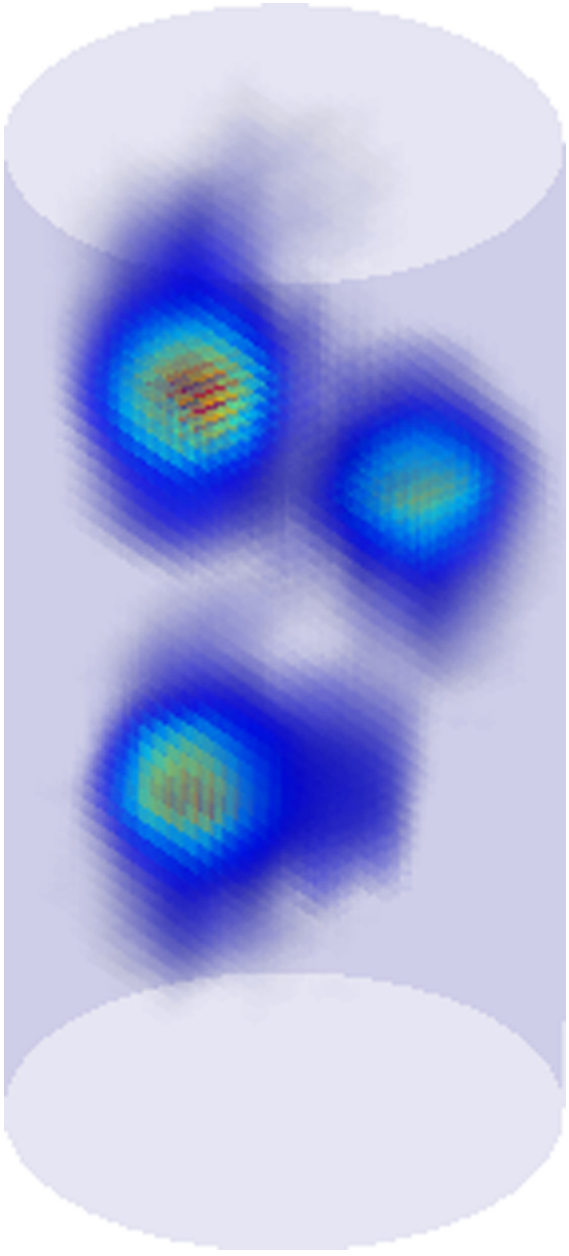

Fig. 9. Reconstructed 3D volume showing ^{137}Cs activity in the drum. Note that the image has been interpolated on a finer grid. The drum outline is shown for illustration.

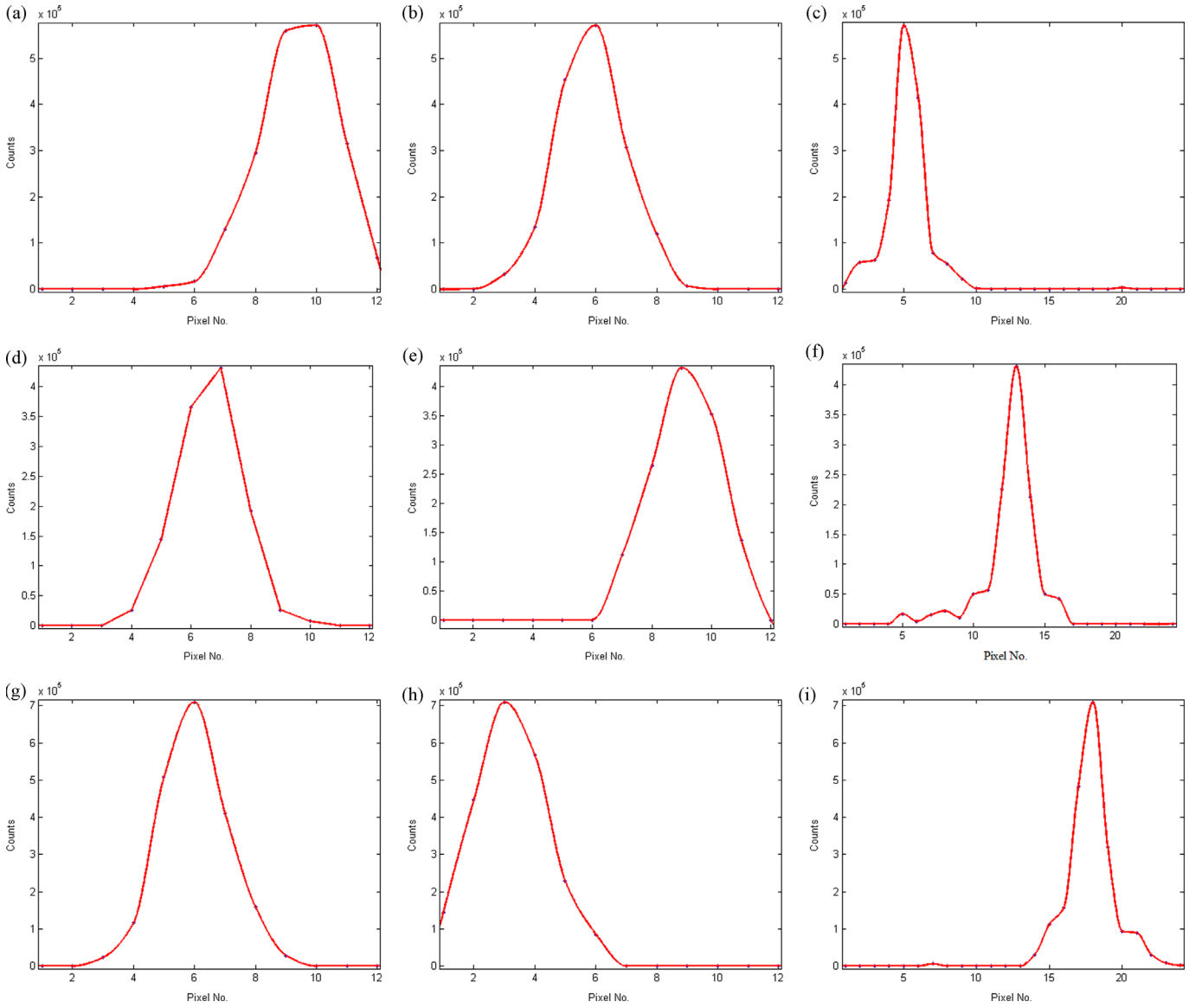

Fig. 10. Intensity profile along *x*-axis, *y*-axis and *z*-axis respectively for Source A (a–c), Source B (d–f) and Source C (g–i).

of the important factors of image degradation in SPECT. Deconvolution methods may be applied on the obtained images to reduce the blurring effect. However, it can be seen from these results that even without any correction for collimator blurring, it is possible to locate the radioisotopes with reasonable accuracy.

3. Conclusion

3D SPECT imaging facility has been developed at Purnima Labs, BARC for characterization of waste drums. The focus of this paper is on using $LaBr_3$:Ce detectors for imaging of waste drums which often have radioisotopes with have closely spaced gamma peaks like in ^{239}Pu. Preliminary experimental results have been discussed showing the application of the technique in finding out the 3D activity distribution in a dummy waste drum using $LaBr_3$:Ce detectors. Future work will focus on applying this technique for heterogeneous matrix with ^{239}Pu sources and finally testing with actual waste drums.

References

[1] F. Natterer, The Mathematics of Computerized Tomography, Wiley, New York, 1986.
[2] A.C. Kak, M. Slaney, Principles of Computerized Tomography, IEEE Press, 1987.
[3] Glenn F. Knoll, Radiation Detection and Measurement, 3rd ed., Wiley, New York, 2000.
[4] ⟨www.detectors.saint-gobain.com/uploadedFiles/SGdetectors/Documents/Technical Information Notes/BrilLanCe-Scintillators-Performance-Summary.pdf⟩.
[5] R.G Novikov, An inversion formula for the attenuated X-ray transformation, Arkiv foer Matematik 40 (2002) 145–167.
[6] L.A. Kunyansky, A new SPECT reconstruction algorithm based on the Novikov explicit inversion formula, Inverse Problems 17 (2001) 293–306.
[7] Roy Tushar, Sarkar P.S Sinha Amar, Simulation study of single photon emission computed tomography for industrial applications CT2008, tomography confluence, in: Proceedings of the AIP Conference , vol. 1050, 2009.
[8] L.A. Feldkamp, L.C. Davis, J.W. Kress, Journal of the Optical Society of America 1 (1984) 612–619.